

Investigation of corrosion minimization in integrated circuit assemblies

by

Gordon F. Davis Jr.

A thesis submitted to the graduate faculty
in partial fulfillment of the requirements for the degree of
MASTER OF SCIENCE

Major: Materials Science and Engineering

Program of Study Committee:
L. Scott Chumbley, Major Professor
Brian Gleeson
Kurt Hebert

Iowa State University

Ames, Iowa

2002

Copyright © Gordon F. Davis Jr., 2002. All rights reserved.

Graduate College
Iowa State University

This is to certify that the master's thesis of

Gordon Francis Davis Jr.

has met the thesis requirements of Iowa State University

A small, dark, and heavily redacted mark, likely a signature, located in the lower-left quadrant of the page.

Signatures have been redacted for privacy

TABLE OF CONTENTS

LIST OF FIGURES	iv
LIST OF TABLES	vi
ACKNOWLEDGEMENTS	vii
CHAPTER 1. INTRODUCTION	1
Statement of Work	1
General Overview	1
Life Expectancy Prediction	6
Accelerated Stress Testing	9
Corrosion of the Metal Surface	10
CHAPTER 2. EXPERIMENTAL PROCEDURE	13
Material Selection	13
Ionic Extraction and Measurement	14
Device Preparation	15
HAST Testing	19
CHAPTER 3. EXPERIMENTAL RESULTS AND DISCUSSION	22
Sample Size	22
Ionic Content Measurement	22
HAST Testing	23
Internal Device Analysis Results	30
Internal Device Analysis Discussion	38
CHAPTER 4. CONCLUSIONS	42
Future Research	42
REFERENCES	43
APPENDIX	46

LIST OF FIGURES

Figure 1. Schematic Representation of a Plastic Ball-Grid-Array Package	2
Figure 2. Schematic Representation of a Hermetically Sealed Ball-Grid-Array Package	3
Figure 3. Reduction Trend in Extractable Ion Content	4
Figure 4. Improvements in the 85°C/85% RH Performance in Plastic-Packaged CMOS ICs	5
Figure 5. Reliability of Electronics Systems – “Bathtub Curve”	7
Figure 6. Corroded Aluminum Bond Pad, 546X Magnification	11
Figure 7. Parr Extraction Chamber (Extraction Bomb)	14
Figure 8. Six Analog Devices Inc. ICs Populated Within the 846B MCM	15
Figure 9. Diagram of CMP04 IC Die Connections, 100X	16
Figure 10. Diagram of AD713 Integrated Circuit Die Connections, 100X	16
Figure 11. Diagram of AD598 Integrated Circuit Die Connections, 100X	17
Figure 12. Wire-Bonded Assembly of the 846B MCM Prior to Encapsulation, 2X	17
Figure 13. Underside of Test Package Indicating Solder Bump Configurations, 1X	18
Figure 14. HAST Chamber	20
Figure 15. HAST Test Board for the 846B MCMs	21
Figure 16. Device Failure Rate Encapsulated with Sample LD (Control)	24
Figure 17. Device Failure Rate Encapsulated with Sample LD7	25
Figure 18. Device Failure Rate Encapsulated with Sample LR	27
Figure 19. Device Failure Rate Encapsulated LA1	29
Figure 20. All Sample Encapsulant Comparison Failure Rate	30
Figure 21. Device Coated with a Sample Encapsulat, 10X	31
Figure 22. Plasma Etcher and Regulator Model Plasmod GCM100	32
Figure 23. SEM Picture of Representative Bond Pad Corrosion on Sample LD-2	33
Figure 24. SEM Photo of Representative Corrosion Free Bond Pad on Sample LD-2	33
Figure 25. SEM Photo of Representative Corroded Bond Pad on Sample LD-5	35
Figure 26. SEM Photo of Representative Corrosion Free Bond Pad on Sample LD-5	35
Figure 27. Typical Bond Pad Corrosion of Sample LR-4	37
Figure 28. Typical Bond Pad Corrosion of Sample LR-5	37
Figure 29. Electromigration Growth on the BGA Solder Bumps, 20X	46

Figure 30. Encapsulant Leakage from Reversion, 10X

47

LIST OF TABLES

Table 1. Sample Identification	13
Table 2. Bias Connections Used During HAST Exposures of the Demonstration Vehicles	21
Table 3. Ionic Extraction Data	23
Table 4. Corrosion-Free Bond Pads, Sample LD-2	34
Table 5. Corrosion-Free Bond Pads, Sample LD-5	34

ACKNOWLEDGEMENTS

I would like to thank the following Rockwell Collins peers, mentors and managers: Phil Krotz for the inspiration to start the graduate program; John Hagge and Nicole Cavanah for providing mentoring and leadership, without these two, all of this work would not have been possible; all my Application Engineering team members and members of the Component and Materials Evaluation Lab for all their assistance and support; Chad Morgan, a former Materials and Processes team member, for sharing the ride to Ames with me every week for class.

I am appreciative of my major professor, Dr. Scott Chumbley and the other professors on my advisory committee; Professor Brian Gleeson and Professor Kurt Hebert. I would like to specifically thank Scott for his guidance and assistance in completing the graduate program.

Finally, I would like to thank my family. First, my parents for the values and lessons they taught me throughout the years. Without them, I would not have been in the position to achieve my accomplishments in life. Finally, my wife, Melanie, who has provided me with all the support I needed to complete this goal.

CHAPTER 1. INTRODUCTION

Statement of Work

Studies have shown that a major contributor to commercial-off-the-shelf (COTS) integrated circuits (ICs) package failures in harsh environmental conditions used for high reliability applications is the encapsulating material. In specific, the corrosion mechanism resulting from chlorine ions residing within the encapsulating material, acting in conjunction with moisture and an electrical bias, to cause failures. This work serves to investigate the reduction of corrosion propagation, which leads to failures at the gold/aluminum bond pad interface on the IC. The project entailed the use of various newly-formulated encapsulating compounds with reduced levels of chlorine content, while maintaining consistent levels of bromine and sodium. It is the intent of this work to identify the maximum chlorine ionic content allowable that results in no corrosion or very slow propagation of corrosion at the IC bond pad. While the corrosion mechanism is well understood in, this work is unique because the maximum threshold of allowable chlorides is under investigation. This study was completed to advance industry knowledge concerning the use of COTS components as direct replacements of hermetic parts used in extreme conditions.

General Overview

The declining availability and higher cost of high-reliability ceramic packaged or hermetically sealed ICs has dramatically affected manufacturers of military, aerospace and other high-reliability electronics. Designers of these products have been pressured both by price and availability to incorporate COTS plastic encapsulated microcircuits (PEMs) in their designs. A specific case of increase in the military's use of COTS electronic components was illustrated by the "Perry Memo" in 1994 [1]. The major driver for this action was cost; a hermetic component can cost 10 or more times the equivalent COTS component [1].

For the purposes of this work, high reliability and harsh environmental conditions definitions as defined by Rockwell Collins and/or indicated by their customers are as follows:

- High reliability – applications where flight or life critical equipment are essential and injury or death may result if unexpected failures occur
- Temperatures ranges from -65°C to an excess of 200°C – this is attributed to aircraft which fly above 30,000 feet altitude, electronics equipment located outside the pressurized environment, dormant aircraft sitting on hot sunny runways in tropical regions, and electronics used for aircraft engine controls
- Humidity at 100 percent – this is common when flying in all-weather conditions, and aircraft which land from cold, high altitude conditions into tropical humidity conditions
- High salt concentration - equipment exposed to high salt concentrations as experienced aboard naval aircraft and vessels

COTS PEMs (Figure 1) offer a number of advantages over the hermetically sealed/ceramic packages (Figure 2):

- Cost
- Availability
- Greater component variety
- Lighter weight smaller packaging

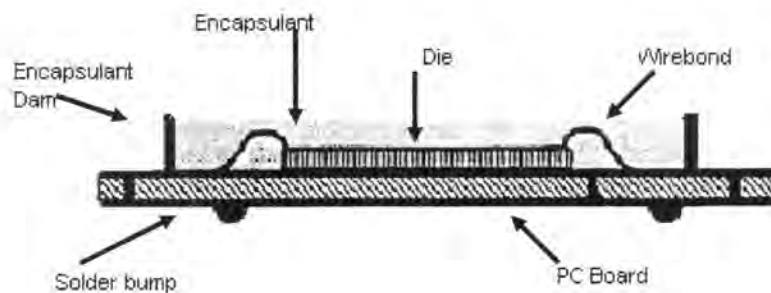


Figure 1. Schematic Representation of a Plastic Ball-Grid-Array Package

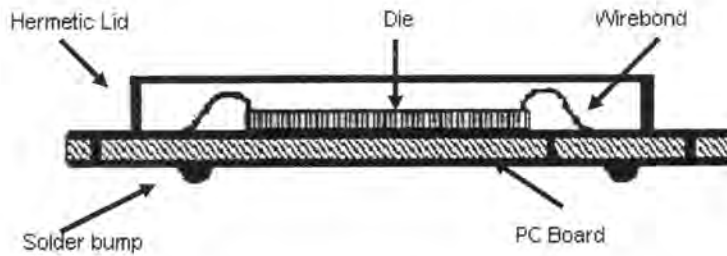


Figure 2. Schematic Representation of a Hermetically Sealed Ball-Grid-Array Package

The use of COTS components with unacceptable plastic encapsulation and/or poor manufacturing techniques can present reliability risks in military, aerospace and life support equipment that are not experienced with hermetic devices [2, 7]. These risks include [2]:

- Delamination - separation of the encapsulant from the surface of the die
- Popcorning - cracks that result from sudden vaporization of absorbed moisture
- Internal corrosion – corrosion at the wire bond pad interface on the die

Many feel the likelihood of corrosion occurring in field components today is insignificant based on advances in cleaner processing, passivation integrity, mold compound purity and encapsulation adhesion over the last several years [8]. These advances have been toward commercial reliability standards and not high reliability goals. It has been shown in several studies that corrosion is a primary failure mechanism [24, 25] for components that are required to meet extended life requirements in harsh end use conditions.

High reliability components require encapsulants that minimize the potential for internal corrosion caused by chlorine ions. Hermetic sealed packages have corrosion protection for two reasons: chlorine ions are not present internally in the semiconductor package because an epoxy encapsulant does not exist, and the components are sealed to prevent absorption of moisture from the environment.

Before epoxy encapsulants were developed for use in the 1960's, phenolic molding compounds were used to encapsulate IC. This material led to considerable

corrosion of the IC when subjected to high humidity environments. This was attributed to the high levels of ionic content within the encapsulant material, specifically chlorine ions. Epoxy encapsulants were introduced in the 1960s which improved reliability by reducing ionic content levels to as low as 0.04 percent, or 400 parts per million (ppm). This is a tremendous amount of content by today's high purity standards of 10 ppm [22]. Continual improvements to the encapsulant materials were made and by the early 1970s values of 100 ppm range were common [22]. These new materials lead to substantial reliability improvements, which drove further material advances. By the late 1980s, typical compounds had chlorine levels less than 30 ppm [22]. Manufacturers of high reliability electronics were using encapsulants with less than 10 ppm extractable chlorine [23]. This is typical of present day chlorine levels. The reduction of ionic content in encapsulants over time is illustrated in Figure 3 [22].

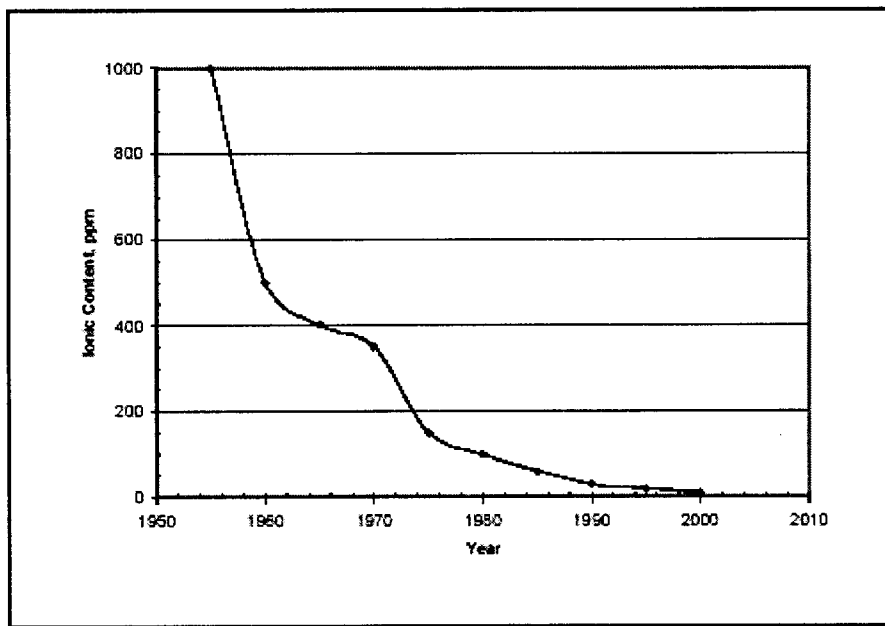


Figure 3. Reduction Trend in Extractable Ion Content

Additional evidence is illustrated in Figure 4 [7], which relates HAST failure rate to year of production. This coincides with the data from Figure 3. The reduction of ionic

content (mainly chlorine) in the encapsulant material was deduced to be essential to increase life expectancy. However, an additional item that improved reliability is highlighted in Figure 3. This is continuous improvement of the package build process which leads to increased life expectation of plastic encapsulated parts.

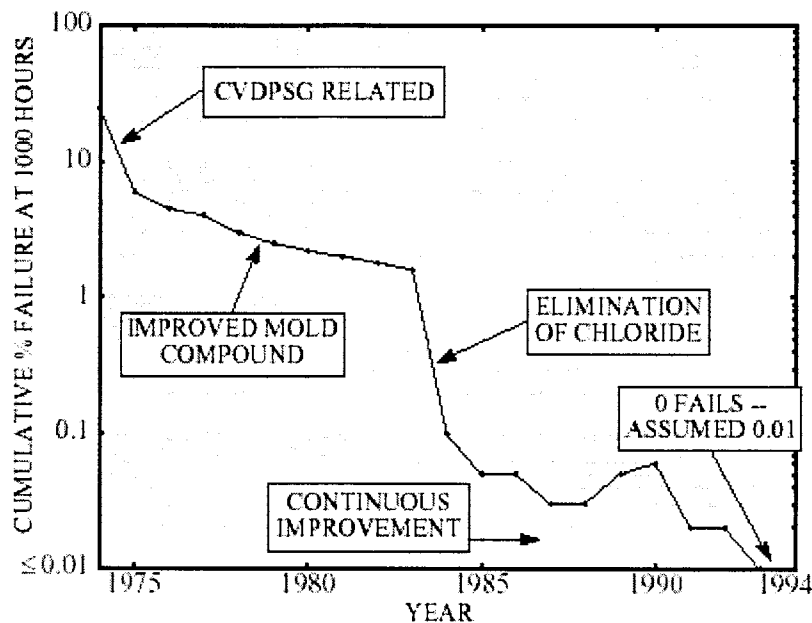


Figure 4. Improvements in the 85°C/85% RH Performance in Plastic-Packaged CMOS ICs

The material selection for encapsulation is essential in developing COTS PEMs for use in high reliability applications. The proper material selection must provide adequate mechanical strength and a means of minimizing the potential for delamination, popcorning and, most importantly, corrosion caused by high levels of chlorine ions transported by permeation of moisture through the encapsulation material.

Two main resin systems currently used for encapsulating electronic parts are silicone and epoxy. Silicone encapsulants have high purity and low ionic content and they provide good corrosion protection. However, they typically have a very high coefficient of thermal expansion (CTE) and provide little mechanical protection to the wire-bonds and die. For this reason silicone was not considered an acceptable material for further

investigation in this research. Epoxy encapsulants provide excellent mechanical protection, but they are difficult to manufacture with low levels of chlorides. The chlorine ions are very common in the chemicals used in processing PEMs, and they are also by-products of the encapsulant resin [13].

Life Expectancy Prediction

High reliability life predictions are difficult to estimate when conditions such as extreme temperature and high humidity exist. Figure 5 [24] illustrates typical failure rates (such as might be common in a communication device employing IC circuits) as a function of life. Three distinct regions of varying failure rates for the assembled system are seen, due to different failure mechanisms. This is important to understand based on the fact that system failures are due to sub-system failures which, in turn, are due to specific IC device failures. It is to a specific device failure mechanism, namely, corrosion of the contact leads for an IC device, that this thesis is directed.

As observed in Figure 5, the “infant mortality” failures come from manufacturing defects, which can be minimized by optimizing and controlling the assembly process. The second failure mechanism shown is “early wear out”. These failures are typically related to defects in raw material and are unpredictable. The final failure mechanism is “strong wear out”. These failures are typically related to mechanical wear out, corrosion, etc. These are the failures of interest for this study. If corrosion can be minimized, the “strong wear out” failure rates would be minimized, thus extending the life of the device, and the entire system.

Electronic systems are characterized by three regions in the failure rate vs. time graph:

- **Infant mortality**
 - Failures due primarily to serious manufacturing defects.
- **Useful life**
 - Failures caused by defects or early wear-out.
- **Strong wear-out**
 - Failures caused by fundamental wear-out mechanism corrosion, fatigue....

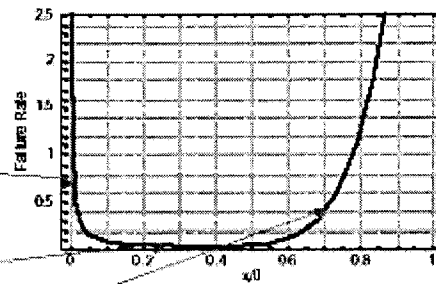


Figure 5. Reliability of Electronics Systems – “Bathtub Curve”

Many device manufacturers use predictive models to provide the customer with relative life expectancy, reliability of their products, and general suitability of the devices for certain applications. This data is required when selecting components for the end-use application. Predictive models factor such things as temperature, humidity and electrical bias effects on the component. Many models are used, but only three will be discussed here due to the relevance related to this thesis. First, the Arrhenius Relationship provides a life expectancy model as a function of temperature. This is an exponential decay model that is used to derive acceleration factors for devices required to operate in high temperature environments and is as follows [17, 18]:

$$A_f = \text{Acceleration Factor} = \exp[E_a/k \cdot (1/T_u - 1/T_t)]$$

E_a = Activation energy, typical value for a given failure mechanism
or derived from empirical data

k = Boltzman's Constant (8.6171×10^{-5} eV)

T_u = Use environment junction temperature (in K)

T_t = Test environment junction temperature (in K)

The second model is the Hallberg-Peck model. This model provides a means to derive life expectancy of a component as related to stresses caused by temperature, humidity and bias. This model is used for HAST testing performed with and without a bias applied to the part and is as follows [20]:

$$A_f = \text{Acceleration factor} = (RH_t/RH_u)^3 \cdot [E_a/k \cdot (1/T_u - 1/T_t)]$$

RH_t = Test environment relative humidity

RH_u = Use environment relative humidity

E_a = Activation energy, typical value for a given failure mechanism

k = Boltzman's Constant (8.6171×10^{-5} eV)

T_u = Use environment junction temperature (in K)

T_t = Test environment junction temperature (in K)

Third, Brizoux, et al [19], developed an equation based on effects from temperature and humidity effects. The use of this model is minimal throughout the industry as compared to the two preceding equations. It is based on Peck's law and the Thompson-CSF model [17]. This equation assumes temperature and power supply voltage (bias) initiate failures in the device and is as follows:

A_f = Acceleration Factor =

$$\exp [0.7/k \cdot (1/T_j - 1/328)] \cdot (RH_h/50)^{2.66} \cdot \exp (V - 1.1V_n)$$

T_j = Junction temperature (in K)

k = Boltzman's Constant (8.6171×10^{-5} eV)

RH_h = Relative humidity at the die surface

V = Power supply voltage (volts)

V_n = Nominal power supply voltage (volts)

These three models provide a prediction of life expectancy and failure, but they do not necessarily provide accurate information for determining PEMs reliability in harsh operating conditions. None of the three models take in account chlorine content contained in the encapsulant material or contaminants introduced in processing the devices. They also fail to account for coefficient of thermal expansion mismatches as well as any effects that drive the corrosion failure mechanism such as ionic content and permeability of the

encapsulant. Due to these reasons, it was crucial that all samples be subjected to HAST. HAST does not represent actual life because of the extreme parameters of the test; it is a test method that is designed to accelerate the corrosion failure mechanism.

Accelerated Stress Testing

Plastic encapsulated packaged ICs are typically qualified using tests that accelerate failure mechanism due to moisture. Two test methods have been predominantly used for such accelerated testing. Both are used by the electronics industry based on components and material requirements. The first, temperature-humidity-bias (THB) testing, is typically done at 85°C and 85% relative humidity for a predetermined time. The time ranges from 168 hours to more than 5000 hours. As encapsulation material and processing methods improved dramatically over the years, this meant an increased amount of time was needed to provide an acceptable number of failures to measure. THB testing became unacceptably time-consuming to manufacturers. As a result, the highly accelerated stress test (HAST) was developed and is now used as the test method of choice for accelerating the corrosion mechanism.

HAST is performed at high temperature (130°C), high relative humidity (85%), with an applied bias and typically under higher than atmospheric pressure conditions (i.e., 30 lb/in²) to accelerate the penetration of moisture through the encapsulant material. HAST is intended to accelerate the bond pad corrosion mechanism that leads to device failure [15]. This study employed HAST testing at 130°C, 85% relative humidity, a 5V applied bias and at 19 lb/in². The pressure was less than 30 lb/in² due to the limitations of the chamber. For a PEM device to be considered equivalent to a hermetic package in terms of long term reliability in harsh applications, the COTS package must be able to withstand 1000 hours of HAST exposure and maintain acceptable operating parameters of less than 5% failure rate. The preparation and testing will be discussed in further detail within the paper.

Corrosion of the Metal Surface

Almost all plastic materials used in electronic packaging absorb moisture. All are water permeable to some degree and allow vapor to pass through the encapsulant to the semiconductor and bond pad. Today's typical plastic molding compounds are reported to have moisture diffusion coefficients around 10^{-6} cm²/sec [3]. The encapsulated component absorbs as much moisture as it will hold for that environmental relative humidity usually within a day or less in some cases [13]. Moisture absorption results in some moisture related failure mechanisms that are not experienced in properly sealed hermetic packages.

Moisture alone has relatively little affect on the reliability of the product. In order to have corrosion, three conditions must be present simultaneously [3-5]:

- There must be moisture or another electrolyte that assists the movements of ionic contaminant
- There must be a voltage gradient either from the circuit or from a galvanic potential developed by the presence of dissimilar metals
- There must be ionic contaminant – the most common ionic species is chlorine that came from the environment, encapsulant or manufacturing process

It can then be assumed that corrosion prevention is possible by eliminating one of the conditions. The most cost effective solution to minimizing corrosion failures is to formulate a material that has minimal or no chlorine content. It is important to add that the manufacturing process must be optimized along with the encapsulant to reduce the introduction of chlorine contamination.

Figure 6 illustrates the corrosion that occurs once chlorine contaminants reach the die bond pad surface. The corroded aluminum pads have a “dried mud flat” appearance that occurs when aluminum is converted to aluminum hydroxide, a material that is gelatinous in form at high humidity. When the gelatinous aluminum hydroxide dries, the cracked segments appear. Corrosion failures resulting in open circuits and detached wire bonds occur predominantly at the areas with the shortest path to the semiconductor die

surface. Moisture absorbs through the areas of highest exposure to the environment, i.e., top or bottom of the device (PEM). The balance of the absorption occurs along the interfaces between the epoxy encapsulant and the lead frame onto the bond wires and eventually to the surface of the die [9].

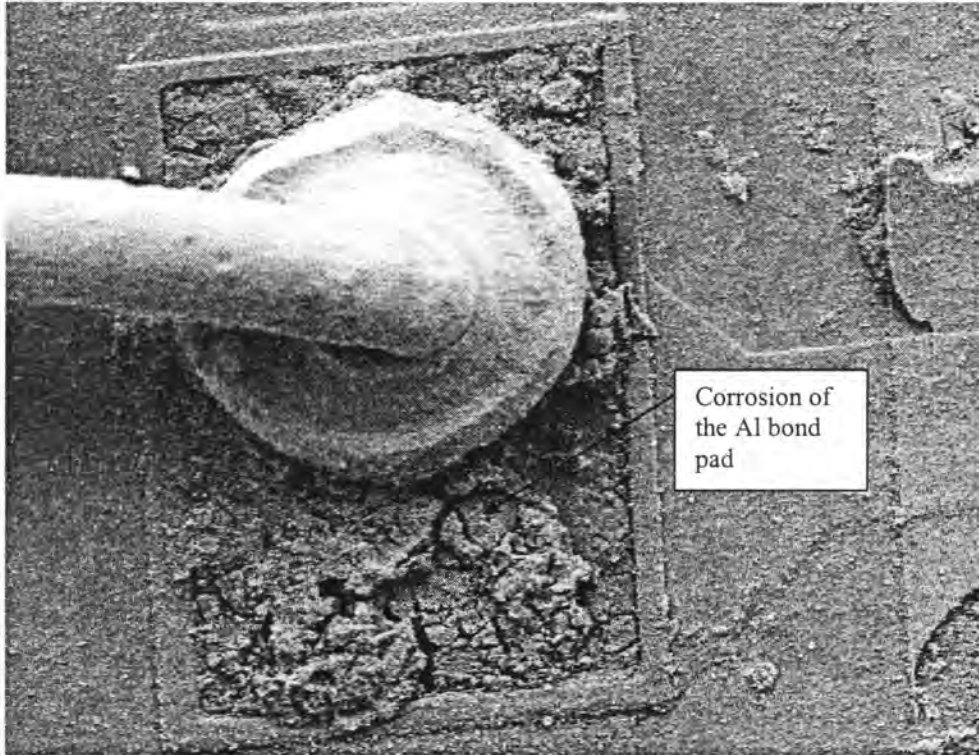
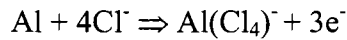


Figure 6. Corroded Aluminum Bond Pad, 546X Magnification

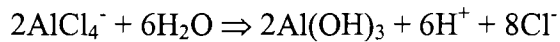
The aluminum corrosion mechanism is well understood and documented [10-12]. The rate of electrolytic corrosion of the die pad interconnect is related to the bias voltage applied to the device, the amount of moisture present, wire bond to pad junction temperature and the electroactivity of the absorbed electrolyte [10-12]. The corrosion mechanism is believed to evolve in the following manner:

- Aluminum oxide is dissolved by the chlorine(Cl) ion, the Cl ion is derived from unstable chlorine residing in unstable structures or excess from byproducts of the encapsulant rein or manufacturing process:

$$\text{Al}(\text{OH})_3 + \text{Cl}^- \Rightarrow \text{Al}(\text{OH})_2\text{Cl} + \text{OH}^-$$
- Once the oxide layer is removed, the exposed aluminum from the die surface reacts with Cl ion:



- The $\text{Al}(\text{Cl}_4)^-$ then reacts with water:



The aluminum corrosion process is regenerative as seen by the presence of chlorine ions in the final resultant of the last equation. The final reaction frees up the chlorine ion to continue the cyclical process as long as moisture is present [8, 14]. The resultant product is aluminum hydroxide $\text{Al}(\text{OH})_3$. The expansion of this structure is enough to crack the aluminum passivation layer of the bond pad as well as degrades conductivity and connectivity on the wire bond to the die bond pad. As a result, small quantities of chlorides can cause significant amounts of corrosion. This mechanism suggests that any amount of chlorines dangerous and will cause corrosion to some extent, but it does not provide insight on amount of corrosion based on chlorides available, and it does not suggest whether the chlorine will preferentially attack a biased bond pad.

CHAPTER 2. EXPERIMENTAL PROCEDURE

Material Selection

This study focused on four encapsulation materials. All materials were developed by Dexter Electronic Materials, now Henkel Loctite Electronic Materials. Only one supplier's materials were tested due to the fact that they were willing to provide prototype materials for high reliability testing. The sample encapsulants included a control encapsulant that is presently used in industry, a new material that has been available for a couple years, and two new formulations. These are listed in Table 1.

Table 1. Sample Identification

Sample ID	Supplier ID	Material Description
LD	FP4450	Control encapsulation, this is a preferred industry standard material for die encapsulation
LD-7	FP4450HF	This formulation has 40% lower ionic content than FP4450
LR	CNB 915-35	"Cleanest Commercial Resin", a duplicate of FP4450HF with the exception that all of the resins in the material have the lowest ionic contamination of any commercial grade resin possible
LA1	CNB 915-36	"Ion Getter", an FP4450HF variation that has a small portion of the filler replaced with an inorganic compound that has a strong propensity to react with and bind chlorine ions

Ionic Extraction and Measurement

An ionic extraction process was performed on all encapsulants used in the study to quantify their level of extractable ionic content. The degree of extractable ionic materials within the plastic packaged IC was measured by the following procedure [26]:

- A cured sample of the encapsulating material is ground to powder and double screened to obtain a sample that passes #80 mesh but not exceed #200 mesh.
- 1 gram of the screened powder and 30 milliliters of distilled or deionized water is placed in a Teflon-lined Parr extraction chamber (Figure 7).
- The Parr extraction chamber is placed in a 160° C oven for 24 hours.
- The extract liquid is filtered through #44 filter paper, and analyzed by Ion Chromatography (ionic content of the extract is reported as ppm to an accuracy of 0.1 ppm for the following: chlorine, bromine, potassium and sodium. This test was done by Huffman Laboratories)

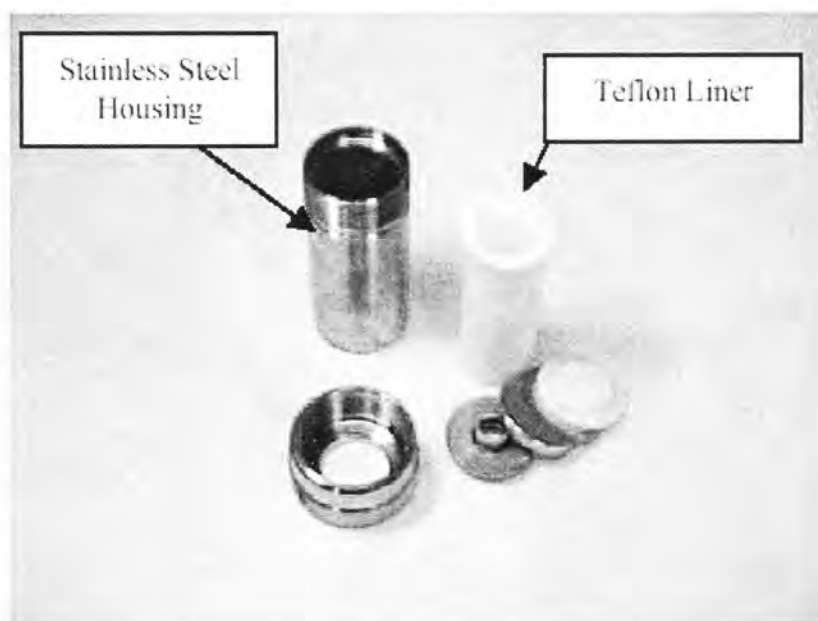


Figure 7. Parr Extraction Chamber (Extraction Bomb)

Device Preparation

The test samples used for this study were part of joint research programs between Rockwell Collins and the Department of the Army. These are:

- Wafer Applied Sealant for PEM Protection (WASPP)
- Robust Packaging of Commercial-Off-the-Shelf Integrated Circuits (ROBOCOTS)

The test samples (Figure 8) were designed to duplicate a typical PEMs IC package. The test package was an 846B MultiChip Module (MCM). It is a robust unit under development for remote electronics applications [16]. The MCM was populated with six ICs supplied by Analog Devices Inc. (ADI): three AD713s; two AD598s; and one CMP04, (Figures 9-11). The final wire bonded substrate assembly can be seen in Figure 12.

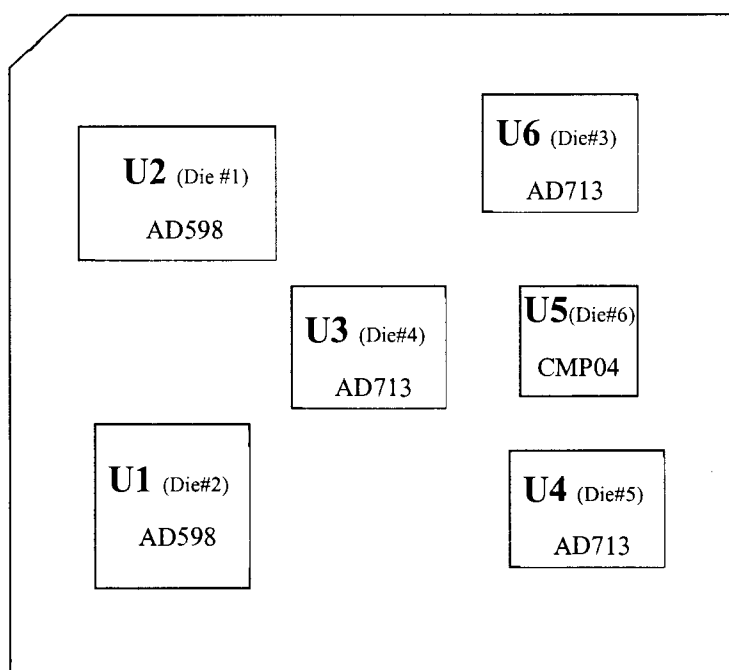


Figure 8. Six Analog Devices Inc. ICs Populated Within the 846B MCM

The MCM was packaged in 0.82 x 0.82 in² Ball Grid Array (BGA) format with 204 signal I/O solder balls on the bottom of the substrate (Figure 13).

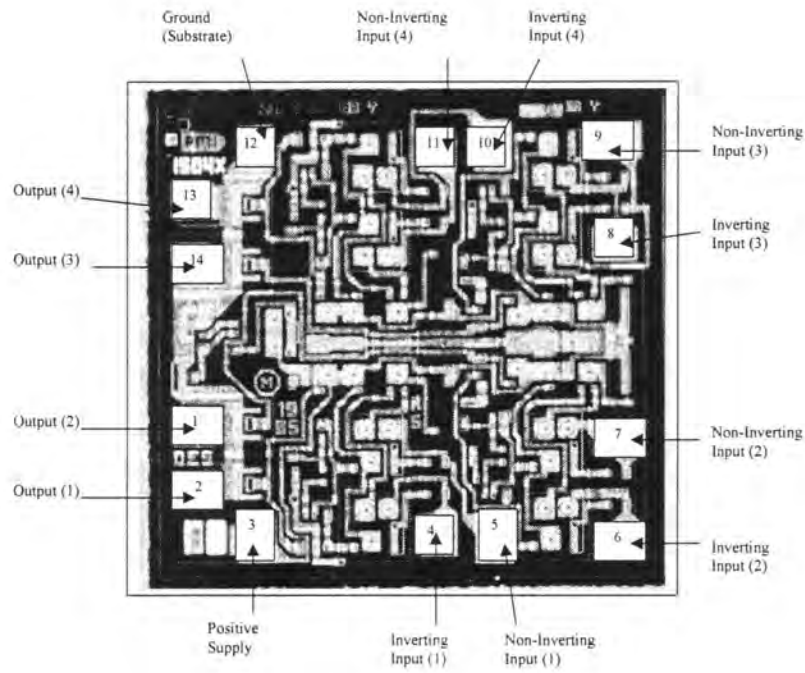


Figure 9. Diagram of CMP04 IC Die Connections, 100X

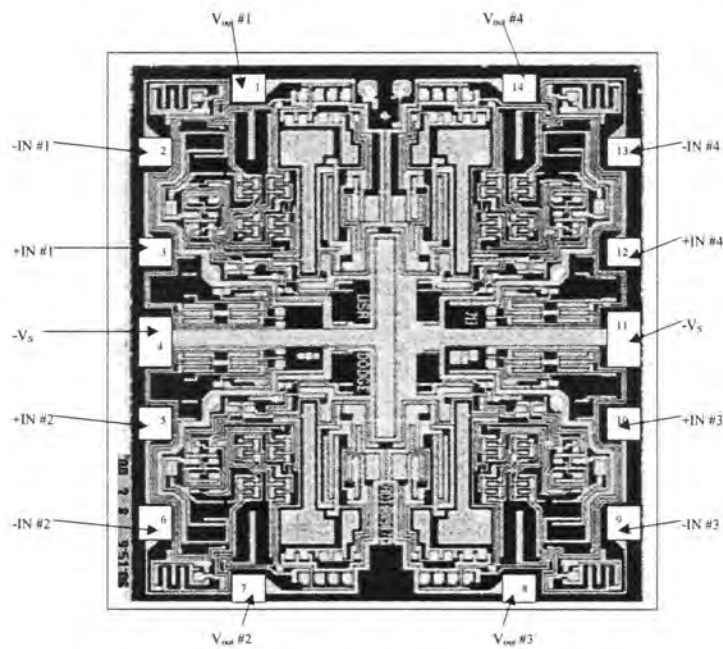


Figure 10. Diagram of AD713 Integrated Circuit Die Connections, 100X

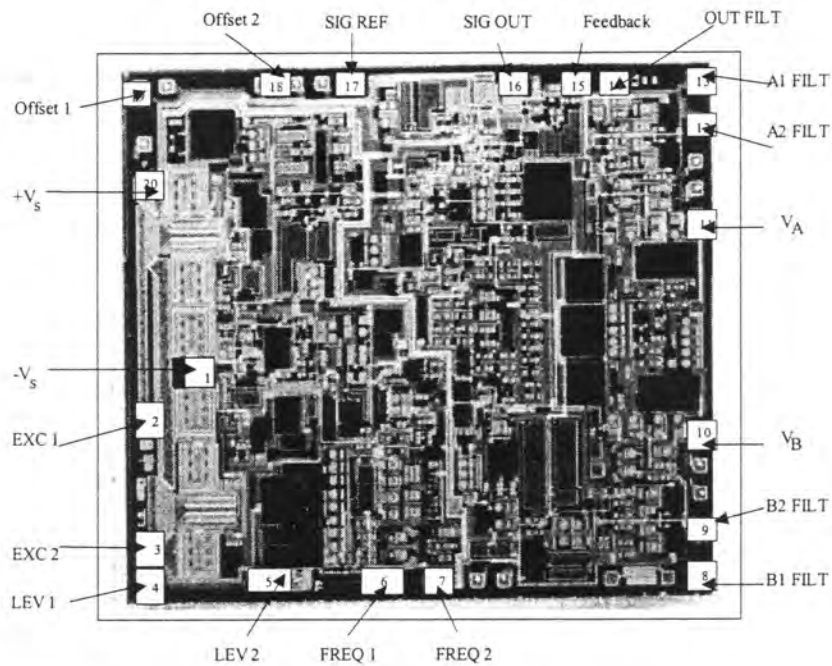


Figure 11. Diagram of AD598 Integrated Circuit Die Connections, 100X

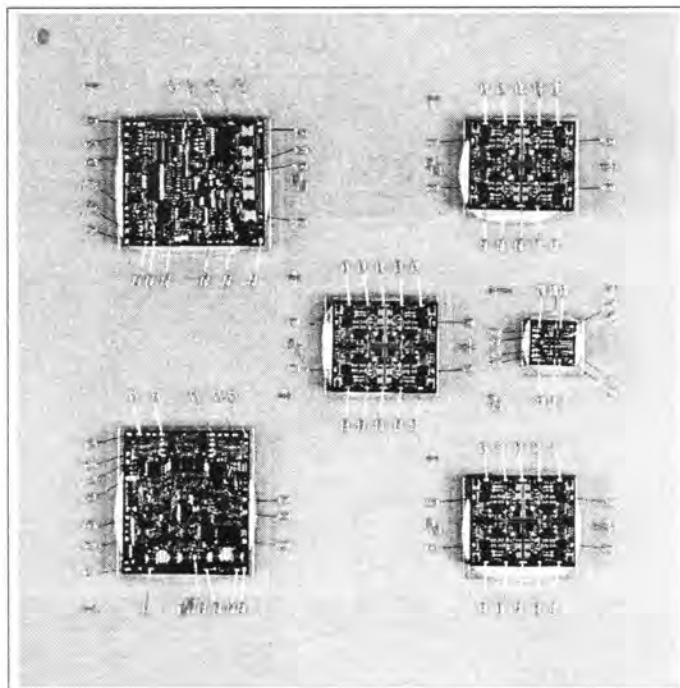


Figure 12. Wire-Bonded Assembly of the 846B MCM Prior to Encapsulation, 2X

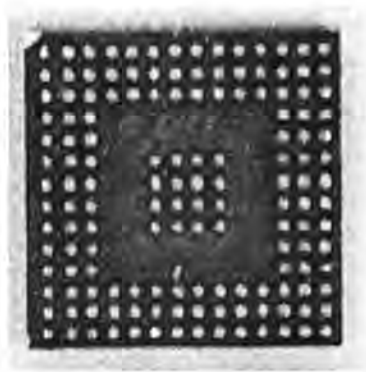


Figure 13. Underside of Test Package Indicating Solder Bump Configurations, 1X

The assembly of the 846B MCM BGA Test Vehicles was accomplished as follows:

- The package substrates (laminate) were cleaned prior to assembly using an ultrasonic cleaner by immersing them in Kyzen Ionox BC solution for 5 minutes, followed by immersion in isopropyl alcohol for 1 minute, followed by rinses in isopropyl and methyl alcohol for 1 minute, and blown dry with nitrogen. Ablestick 84LMI adhesive was dispensed onto the six IC sites on each substrate. Three AD713, two AD598, and one CMP04 were placed.
- The die-bond adhesive was oven cured at 150° C for one hour.
- The substrate assembly was cleaned in an oxygen-ozone plasma for ten minutes to prepare IC bond pads for wire-bonding.
- The ICs were wire-bonded to the substrates with 0.001 inch diameter gold wire using a thermosonic ball wire-bonder operating with approximately 125° C base temperature. Wire-bond pull strengths were tested on each assembly lot. Note: as a minimum, the wire bonds exceeded 4 grams as-bonded and exceeded 3 grams after an aging bake of 125° C for 16 hours.
- A pre-cleaned encapsulant frame was attached to the substrate using 3M VHB adhesive film.
- The dies were encapsulated with a control sample encapsulant and three new formulation encapsulants.

- The cure cycle involved a two-step process of oven cure for 30 minutes at 125° C followed by 90 minutes at 165° C. The step process was done to minimize shrinkage of the epoxy encapsulant.
- Attachment of the eutectic solder balls to the BGA was accomplished by applying flux to the BGA pads. An appropriate stencil was positioned over the pads and solder balls (.025 inch diameter) were vibrationally located into the stencil openings.
- The assemblies were sent through a conveyORIZED SMT reflow oven with a temperature profile appropriate for good solder wetting.
- The finished BGAs were cleaned with a flux removal process (in-line cleaner consisting of Kyzen Aquanox SSA and deionized water).

All three IC die types contained in the BGA were identical to those ICs offered in standard individual PEM products by ADI, so ADI performed the standard production electrical testing on the assemblies. The BGAs were configured so that every wire-bond connection within the BGA had test access through one of the solder bumps on the BGA.

The MCMs were assembled in the Rockwell Collins Advanced Technology Center Microelectronics Lab and the Coralville Production Microelectronics Assembly Area. The PWB laminate substrates were fabricated in the Rockwell Collins Advanced Technology Center Circuit Board Lab.

HAST Testing

The HAST chamber used for testing is depicted in Figure 14. HAST testing of the devices was performed using a 27 socket test circuit board shown in Figure 15. The HAST board was fabricated by Cody Electronics Inc., of Santa Clara, CA. The test sockets are from 3M Textool. Bias connections during HAST exposures provided either minus zero volts (ground) or plus five volts to the various I/O on each IC within the MCMs listed in Table 2.

The MCMs were given pre-conditioning exposures per JEDEC A113 [21], electrically tested again by ADI, and then sent into HAST testing (130°C, 85% Relative

Humidity and 5V bias). The pre-conditioning included a 24 hour bake at 125° C, a moisture soak of 6 hours at 30° C and 60% relative humidity, 3 cycles of infra-red solder reflow at 220° C, a 10 second immersion in flux, and a deionized water rinse. HAST chamber exposure was interrupted for electrical testing in which the MCMs were shipped to ADI for electrical testing after 100, 250, 400, 600, 800, and 1000 cumulative HAST exposure hours.

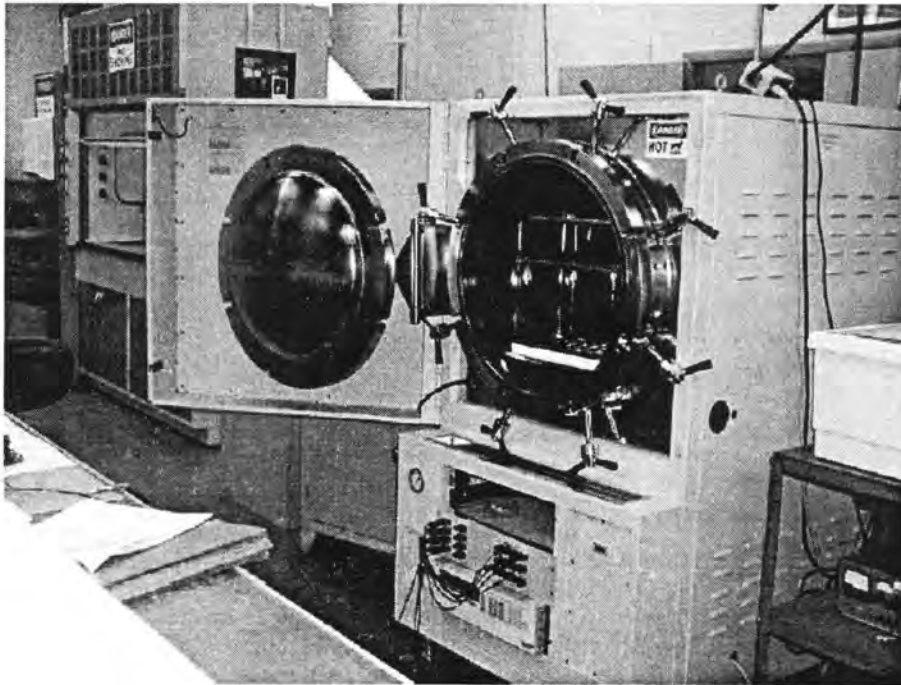


Figure 14. HAST Chamber

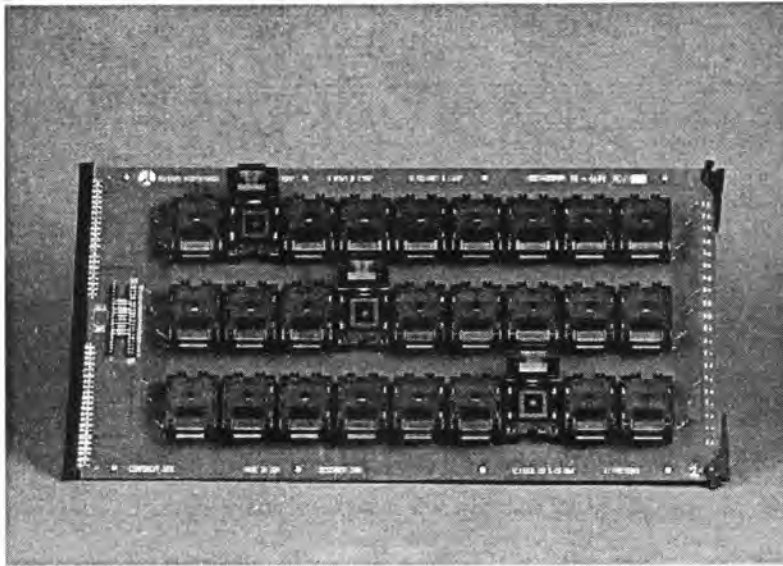


Figure 15. HAST Test Board for the 846B MCMs

Table 2. Bias Connections Used During HAST Exposures of the Demonstration Vehicles

Die Identification	Die Type	Bond Pad	Bond Pad Name	Bias Applied, (-0 = GND)
U1	AD598	10	V(B)	-0
U1	AD598	11	V(A)	+5
U2	AD598	10	V(B)	-0
U2	AD598	11	V(B)	+5
U3	AD713	10	+ Input #3	+5
U3	AD713	9	- Input #3	-0
U3	AD713	2	- Input #1	-0
U4	AD713	3	+ Input #1	+5
U4	AD713	10	+ Input #3	+5
U4	AD713	9	- Input #3	-0
U4	AD713	3	+ Input #1	+5
U4	AD713	2	- Input #1	-0
U5	CMP04	14	Out #3	+5
U5	CMP04	13	Out #4	+5
U5	CMP04	1	Out #2	-0
U5	CMP04	2	Out #1	-0
U6	AD713	10	+ Input #3	+5
U6	AD713	9	- Input #3	-0
U6	AD713	2	- Input #1	-0
U6	AD713	3	+ Input #1	+5

CHAPTER 3. EXPERIMENTAL RESULTS AND DISCUSSION

Sample Size

A total of six BGA packages were encapsulated with each sample encapsulant and each group tested contained the following:

- 6 total dies in each BGA package
- 96 total bond pads in each encapsulated BGA device
- 20 biased bond pads in each BGA: 10 +5 volts and 10 ground
- 576 total bond pads in the lot of 6 BGAs
- 120 total biased bond pads in the lot of 6 BGAs

Failure rates are based on sensitive parameters of the devices. These parameters may fluctuate from the specification limits either before the corrosion mechanism has progressed to cause an actual failure. These failures may occur from absorbed moisture effects, contact resistance variations, etc. Failures attributed to corrosion were associated with mass failures of the electrical measurements due to loss of bond wire adhesion, electrical opens, etc.

Ionic Content Measurement

It is important to note that the test methods for quantifying ionic content are not standardized, and the same material can be characterized with different ppm levels of ionic species depending upon the test method used. Various suppliers and sources report ionic contaminant content by some of the following measures: halide content, chlorine content, bromide content, extractable halide and extractable chlorine content, etc. The method described in Chapter 2 is based on industry publications and recommendations [26].

Ionic extraction (Parr Bomb) was performed on all of the encapsulants in this study to measure and compare the level of extractable ionic contamination. All test sample encapsulant were tested as described earlier. They were tested twice to assess

repeatability. The results of the ionic extractions are listed in Table 3. The specimen testing exhibited reliable experimental repeatability based on the results from Table 3.

Table 3. Ionic Extraction Data

Encapsulant Sample	Na, 1st Run, ppm	Na, 2nd Run, ppm	Cl, 1st Run, ppm	Cl, 2nd Run, ppm	Br, 1st Run, ppm	Br, 2nd Run, ppm
LD	0.6	0.7	3.2	3.6	<0.2	0.3
LD7	0.5	0.4	1.9	1.6	<0.3	<0.3
LR	0.4	0.3	0.9	0.9	<0.3	<0.3
LA1	0.5	0.5	1.4	1.4	<0.3	<0.3

HAST Testing

HAST testing was the testing method selected because it is considered to be the most appropriate test method for determining the ability of the packaged device to resist corrosion. HAST testing was run at 130° C, 85% relative humidity, 18 lb/in² and an electrical bias applied as indicated in Table 2. Four metrics were used to assess failure rates during HAST testing:

1. The percent of electrical test parameters out of limit on dies U1 and U2 within the BGA (the percent out of 10 parameters monitored times 2 ICs/module times the number of modules in HAST exposures)
2. The percent of electrical test parameters out of limit on the U5 die within the BGA (the percent out of 29 parameters monitored times the number of modules in HAST exposures)
3. The percent of operational amplifiers with any of seven electrical test parameters out of limits on dies U3, U4 and U6 within the BGA (the percent out of 4 dies per IC times 6 ICs/module times the number of modules in HAST exposures)
4. A “Failure Index” was calculated as the average of the three percentages listed above. This metric did not include data points that were considered non-corrosion related. These failure types were attributable in some cases to the measured test parameter being just within or just outside of the

established specification limit, electro-migration growths between the solder bumps on the BGA, or to contact resistance variations.

Figure 16 shows the HAST test results for the control group encapsulated with sample LD. There are only a few parameters out of electrical specification parameters after 250 hours of HAST testing. Once the devices had reached the 400 hour exposure mark, all three die types experienced increased electrical failures. By about the 800 hour exposure point the AD713 dies experienced anywhere from thirty-five to sixty percent electrical parameter failures. The AD598 and CMP04 dies experienced a much lower electrical parameter failure rate (about fifteen to eighteen percent). The AD713 dies may be exhibiting different failure rates as compared to the AD598 and CMP04 dies due to the fact that the AD713 die is a more sensitive electronic device. This is evident in Figures 17 – 19 as well.

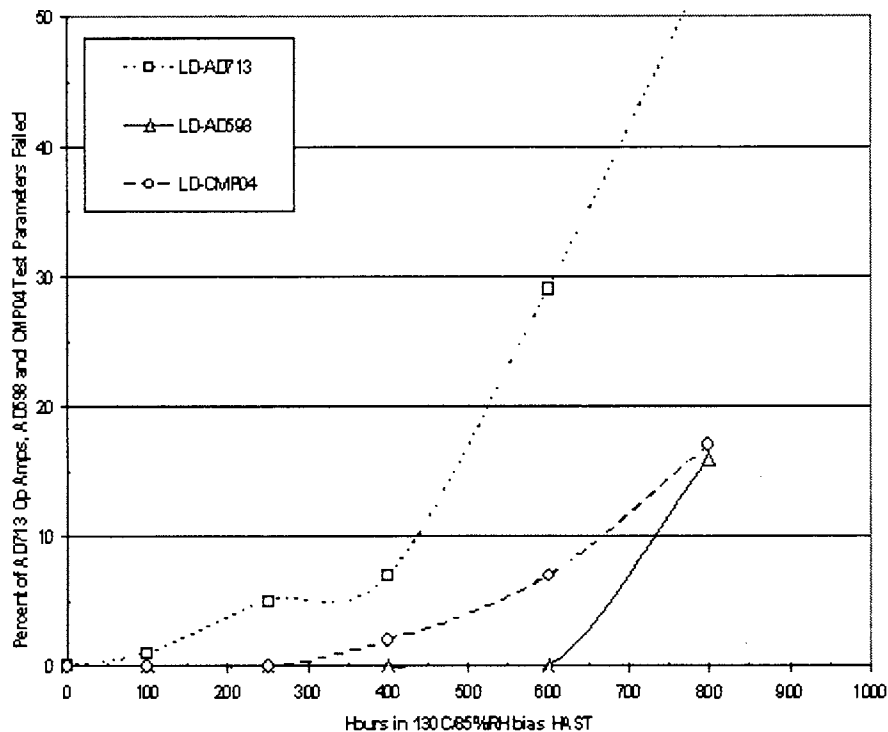


Figure 16. Device Failure Rate Encapsulated with Sample LD (Control)

This experimental data shows a significant improvement in the performance of sample LD encapsulated devices over results of investigations performed a few years ago [15]. Previous experimental results showed considerable failures prior to 100 hours of HAST. The improvements are attributed to the following: process improvements to reduce the chlorine content by the manufacturer and improved dispensing and curing techniques of the encapsulant. Improved process methods were also used in curing of the encapsulant material as to shelter the sample devices from humidity between the encapsulation process and the curing step to avoid the adding more chlorides.

Figure 17 shows the HAST test results for parts encapsulated with sample LD7. Electrical failures begin here at about 250 hours HAST exposure on the AD713 dies. Massive failures do not begin until the 700 to 800 hour point. By about the 800 hour exposure point, the AD713 and the AD598 dies experienced about 20 percent electrical parameter failures, while the CMP04 dies had a much lower electrical parameter failure rate (eight percent).). The CMP04 dies may be exhibiting different failure rates as compared to the AD598 and AD713 dies due to the fact that the CMP04 die is somewhat of a less sensitive electronic device.

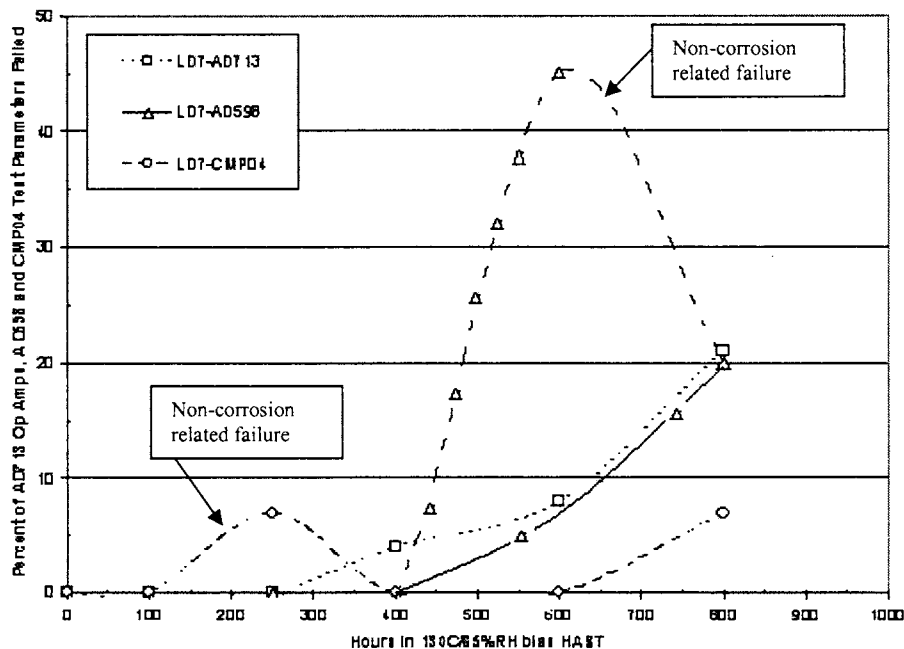


Figure 17. Device Failure Rate Encapsulated with Sample LD7

Sample LD7 encapsulant material contains about 40 percent less chlorine content as the sample LD (control sample) with approximately the same bromide and sodium content levels. The difference in chlorine content between the two materials explains the longer the life of the devices encapsulated with LD7. This can be seen in data comparing Figures 16 and 17, which shows fewer total failures and more hours before failures begin with the LD7 encapsulant. This improvement still did not allow the devices to reach 1000 hours HAST, so the chlorine content threshold must be below 1.9 ppm.

Figure 17 data also shows two non-relevant electrical test failure occurrences, one at the 600 hour mark for the AD598 dies and the second at 250 hours exposure for the CMP04 dies. Both anomalies subside at the next electrical measurement cycle, which leads to the conclusion that these are not attributed to corrosion.

There was also an unexpected issue with sample LD7 encapsulant material. It had reversion or hydrolization problems after the 500 hour exposure point. The material went from a solid state to a liquid form during HAST testing. This caused the samples to be pulled out of testing, thus preventing further electrical testing measurement. Non-corrosion related failures are further discussed in the Appendix. Due to the reversion problem, it is undetermined what the actual hours of exposure could have been. It is believed that the humidity affected the chemistry of polymer bonds thus allowing the material to revert to the liquid state. This problem makes this material unsuitable for high humidity environments.

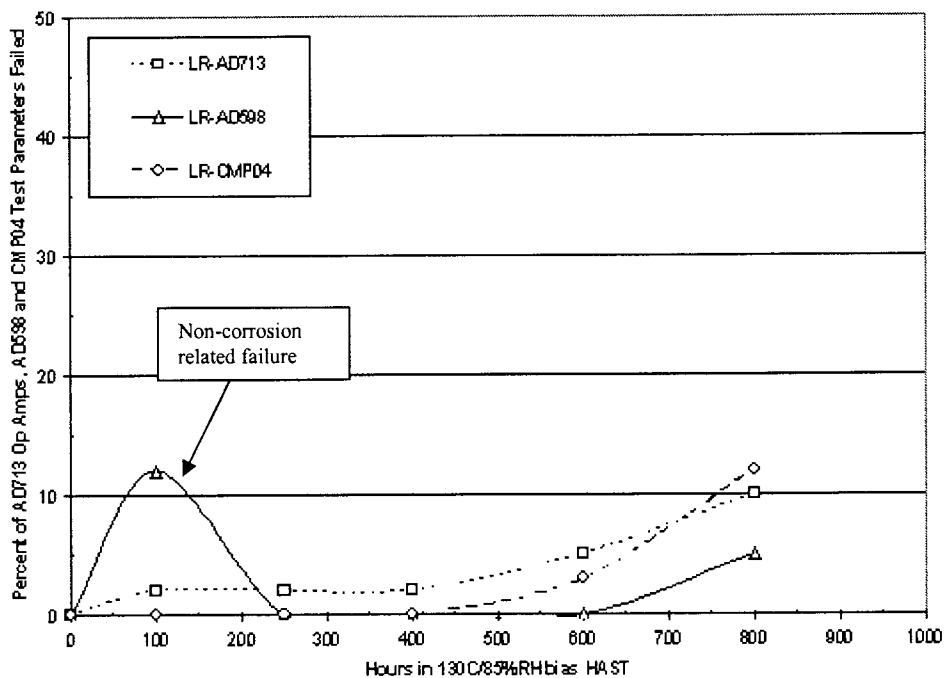


Figure 18. Device Failure Rate Encapsulated with Sample LR

Figure 18 shows the HAST results for sample encapsulant LR. As indicated in Table 3, this formulation contains about half the chlorine ionic content as the LD7 encapsulant and over three times less than the LD material. The sodium and bromides present were also about the same in the three encapsulants. Again, the reduction in chlorine correlates to longevity of these samples. The HAST testing as seen in Figure 18 indicate an improved survival rate, with minimal failures to the 600 hour exposure point. One thing also noted in the data in Figure 18 is the fact that all devices seemed to fail about the same rate where samples LD and the LD7 had certain dies fail sooner than others. One theory would be if the coating does not have a uniform thickness, a die may have less depth of protection, thus allowing moisture to reach the bond pads much easier, which could accelerate the corrosion mechanism. This theory can not be substantiated because the samples were decapsulated and the encapsulation was not measured. This theory needs further study. One experiment to study thickness can be done as follows: BGA packages could be encapsulated with various thicknesses of the sample encapsulant

materials and subjected to HAST. This would provide data to support whether the encapsulant thickness does or does not effect corrosion thus effecting operating life.

There also was a reversion or hydrolization issue with the LR sample encapsulant material. This problem occurred after the 800 hour exposure point. This also caused samples to be withdrawn from further testing thus preventing measurement of electrical parameters for succeeding test intervals. This is shown by the lack of data between 800 and 1000 hours as indicated on Figure 18. Due to the reversion problem, it is undetermined what the actual hours of exposure could have been. This problem makes this material unsuitable for high humidity environments.

There was another example of a non-corrosion failure at the 100 hour point. This resulted from a test socket contact problem for the AD598 die curve. Also, some of the failures that are evident at 800 hrs on the AD598 die curve are due to a solder ball which was damaged and broken off as a result of repeated HAST socket insertion/removals.

Figure 19 shows the HAST results for sample encapsulant LA1. A proprietary material was added to the encapsulant, and according to the manufacturer it functions to bind any chlorine content, thus preventing them from initiating or contributing to the corrosion process. As indicated in Table 3, this formulation contains about 25% less chlorine ionic content as compared to sample LD7 encapsulant and 60% less chlorine than sample LD control encapsulant. Again, the bromide and sodium content is about the same. The HAST data from Figure 19 indicates a moderate improvement compared to the control group of sample LD, but not as significant as expected. This material also shows devices failure rates that do coincide with each other.

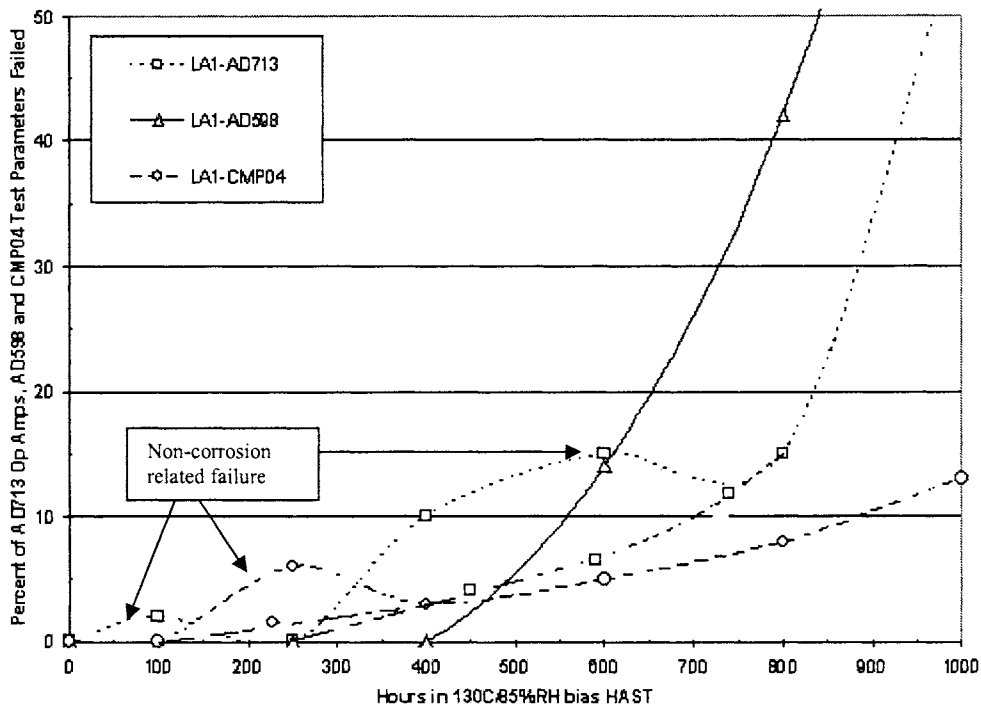


Figure 19. Device Failure Rate Encapsulated LA1

LA1 sample encapsulant also had examples of non-corrosion failures at the 100, 250 and 600 hour mark. These were determined to be electrical anomalies in the package itself, and the data points were discarded because it was not due to corrosion. This material did not have an issue with reversion, which is unexpected since samples LD7 and LR both had this problem. One hypothesis to explain this is the fact that the “ion getter” additive may act as a binding agent in the polymer chain preventing the break down from the saturated water vapor. The chlorine content improvement still did not allow the devices to reach 1000 hours HAST, so the chlorine content threshold must be below 1.4 ppm.

Figure 21 shows the combined failure rate data for all sample materials analyzed. The combined data shows specifically that as the amount of chlorine content is decreased (Table 3) the longer the PEMs last in HAST with the exception to sample LA1. Sample LD7 slightly outperformed sample LA1, even though LA1 less chlorine content. This may be caused from the proprietary material added to LA1. This would require further

investigation. The bromine and sodium contents were essentially the same in all materials tested, so this would indicate that these ionic materials do not play a role in corrosion failures as compared to chlorides. Again, the unexpected issue is the fact that sample LD7 and LR formula are susceptible to reversion and failures related to this phenomenon. The lowest chlorine content improvement still did not allow the devices to reach 1000 hours HAST, so the chlorine content threshold must be below 1.4 ppm. The LR sample had 0.9 ppm, but the reversion problem may have attributed to unaccounted failure mechanisms, so the 0.9 ppm chlorine level can not be considered.

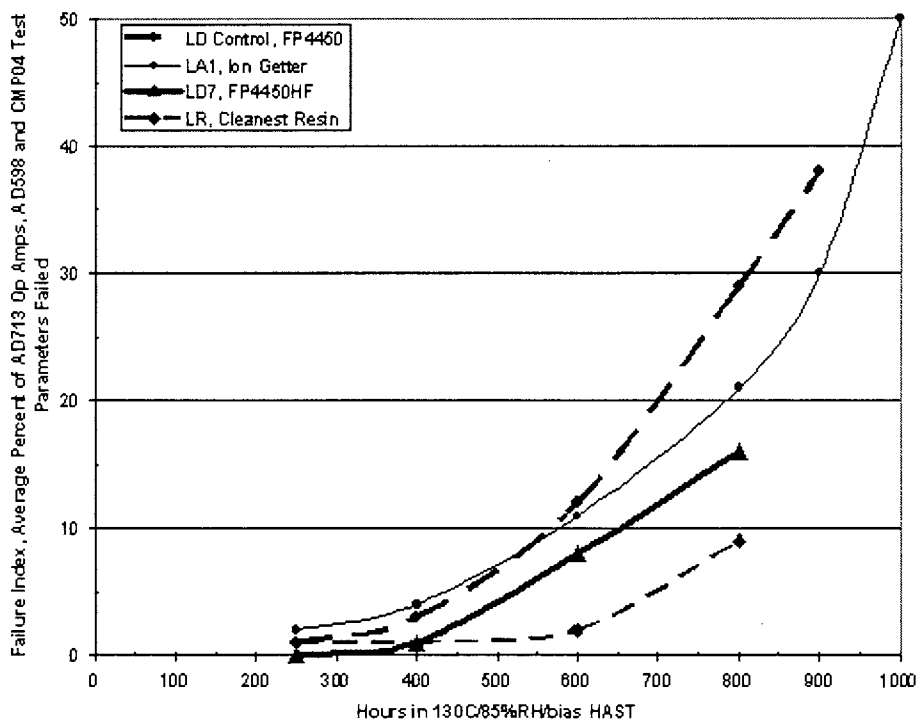


Figure 20. All Sample Encapsulant Comparison Failure Rate

Internal Device Analysis Results

At the end of 1000 hours cumulative HAST exposure (or if 20% failure had been observed), any units which exhibited changes in electrical measurements were subjected to Failure Analysis. The devices were decapsulated, and a scanning electron microscope

(SEM) was used to analyze the bond pads for evidence of corrosion and failure. Two of each sample encapsulant packages were decapsulated for analysis. Only two devices were decapsulated due to time and cost constraints. The packages were decapsulated by the following process:

- Identification labels were removed from the sample PEMs with an exacto-knife.
- The parts (Figure 21) were inserted into a Plasma Etcher and Regulator Model Plasmod GCM100 (Figure 22). Oxygen plasma was used to remove the plastic encapsulation. Oxygen is the only gas used in order to minimize adverse reactions as is commonly experienced in varying degrees using heated acid decapsulation methods; especially in the event of die glassivation breach.



Figure 21. Device Coated with a Sample Encapsulant, 10X

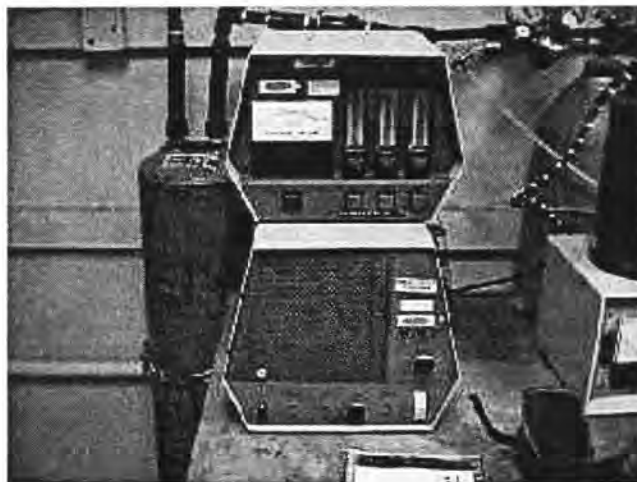


Figure 22. Plasma Etcher and Regulator Model Plasmod GCM100

- RF power was applied and was limited at 15 to 20 watts to ensure that PEMs never subjected to temperatures exceeding 150° C.
- The parts were removed from the plasma etcher twice a day and lightly cleaned with either compressed 1,1,1,2-Tetrafluoroethane or laboratory dry nitrogen to remove degraded epoxy encapsulant.
- The parts were considered complete when the bond pads on the laminate PWB were visible.

Oxygen plasma is used as the standard method for decapsulating and delidding microelectronic parts by both Rockwell Collins and the industry in general. It is a safe, nondestructive process which doesn't damage interconnection patterns, lead bonds or the device itself. Based on results from the Component and Materials Evaluation Lab (CAMEL), oxygen plasma decapsulation has never been known to cause any type of reactions that could be responsible for ball bond to bond pad interface degradation. Thousands of decapsulations have been done over the years at Rockwell Collins using this very standard and controlled method and never has a significant ball bond problem been discovered.

Sample encapsulant LD parts decapsulated were LD-2 and LD-5. Sample LD-2 had considerable corrosion on almost all bond pads as seen in Figure 23. This picture is

representative of the bond pad corrosion on all the devices in the package. Only a few bond pads had no sign of corrosion as seen in Figure 24. Of the bond pads that were not corroded, only two had a positive electrical bias applied and three were -0.0 (grounded) as indicated in Table 4.

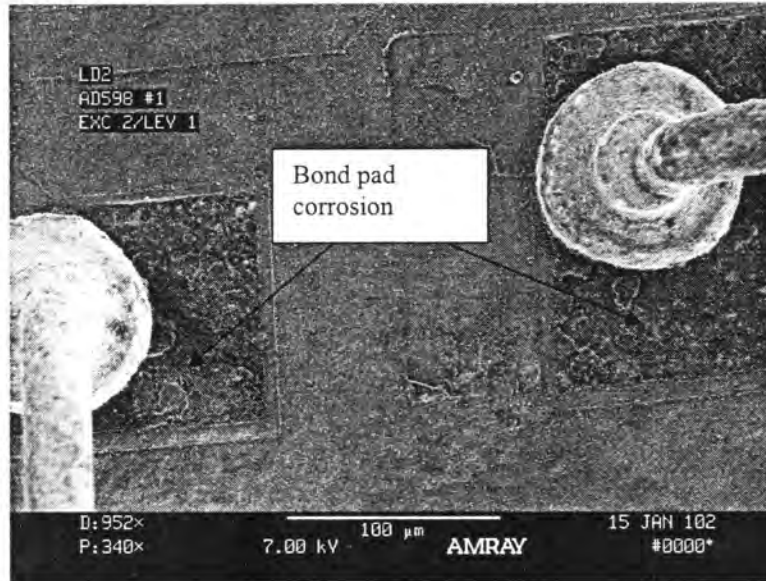


Figure 23. SEM Picture of Representative Bond Pad Corrosion on Sample LD-2

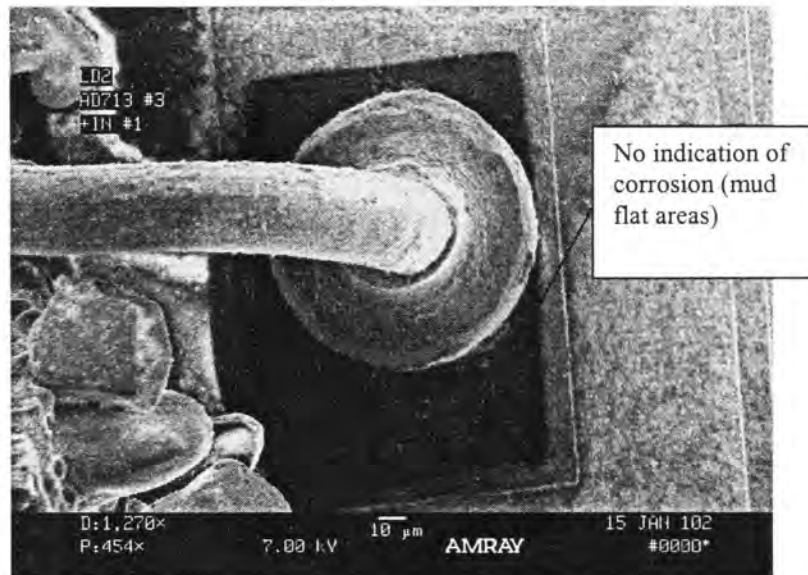


Figure 24. SEM Photo of Representative Corrosion Free Bond Pad on Sample LD-2

Table 4. Corrosion-Free Bond Pads, Sample LD-2

Die	Bias Applied
U2	N/A
U2	N/A
U2	N/A
U2	N/A
U6	N/A
U6	+5
U6	+5
U6	GND
U6	N/A
U3	N/A
U3	N/A
U3	N/A
U3	GND
U3	N/A
U4	N/A
U4	GND
U4	N/A
U4	N/A
U4	N/A

Sample LD-5 also had considerable corrosion on all bond pads with the exception to what is noted in Table 5. This sample does not have any biased pads that are corrosion-free, but only five of the possible 58 total non-biased pads are corrosion free. Typical examples of corroded surface and corrosion-free bond pads can be seen in Figures 25-26.

Table 5. Corrosion-Free Bond Pads, Sample LD-5

IC Type	Bias Applied
U2	N/A
U2	N/A
U2	N/A
U3	N/A
U3	N/A

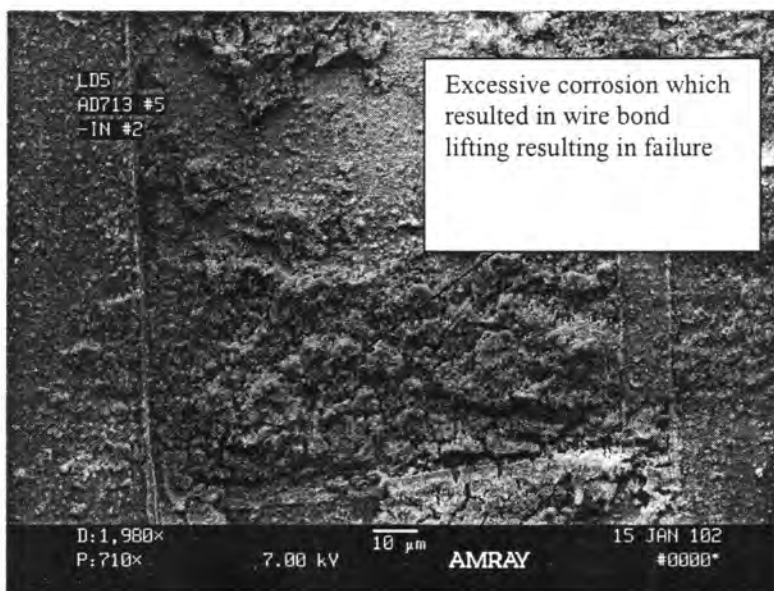


Figure 25. SEM Photo of Representative Corroded Bond Pad on Sample LD-5

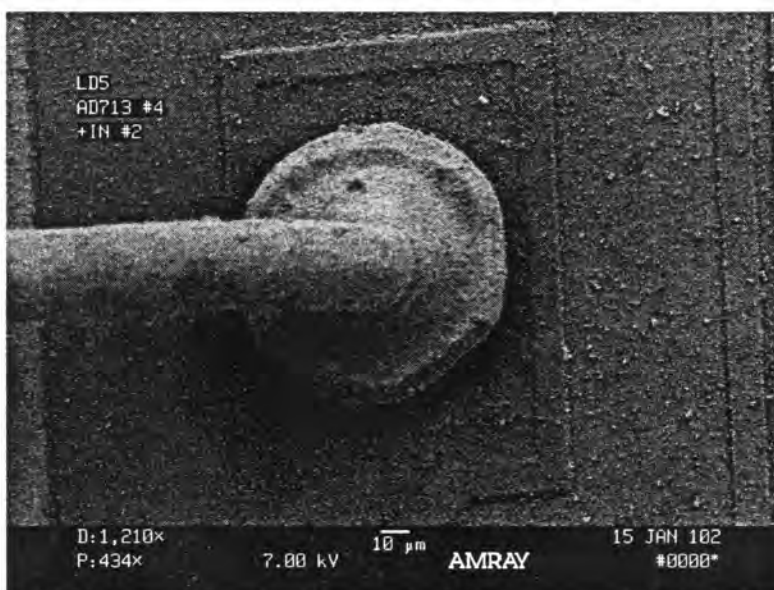


Figure 26. SEM Photo of Representative Corrosion Free Bond Pad on Sample LD-5

LD7 sample parts decapsulated were LD7-3 and LD7-4. This material reverted or hydrolyzed as discussed earlier thus making it very difficult to decapsulate. The material reverted and reset in the test fixture, which made it very difficult to remove without

destroying the samples and test fixture. The samples pulled apart from the laminate substrate when they were removed from the test fixture. The encapsulated dies were glued to a new piece of laminate to decapsulate.

Sample LD7-3 had considerable corrosion on all bond pads. The bond pads for the CMP04 die could not be analyzed because it was lost in the removal process. Sample LD7-4 only contained three die after decapsulation. The AD713 and the CMP04 die were lost in the removal process due to reversion. All bond pads on the dies showed considerable corrosion. The pad analysis on LD7-3 and LD7-4 should not carry as much merit due to reversion. When the epoxy reverted back to a liquid form, the dies were exposed to conditions not accounted for in the onset. Corrosion of the bond pads can not be compared to other samples because of this occurrence.

Sample LR encapsulant parts decapsulated were LR-4 and LR-5. This material hydrolyzed as discussed earlier making it very difficult to decapsulate as well. These samples also pulled apart from the laminate substrate upon removal and had to be re-glued to piece of laminate for the decapsulation procedure. Sample LR-4 had corrosion present on all bond pads. Only three dies were available for analysis, 1-AD713, 1-AD598 and the CMP04. The other dies were missing because they were lost in the removal process. Figure 27 shows the massive corrosion not only on the bond pads themselves, but all over the surface of the die. This is representative of all dies in the decapsulated package.

Sample LR-5 contained all die after decapsulation. All bond pads on the dies also had corrosion present as well, but the corrosion was not as severe as sample LR-4. Figure 28 is representative of the corrosion presence in the package. Corrosion was less severe and focused on the pad and not the surface of the die. The pad analysis on LR-4 and LR-5 should also not carry as much merit due to reversion. As stated above the dies were exposed to conditions not accounted for in the onset. Corrosion of the bond pads can not be compared to other samples because of this occurrence. A note of importance is these parts lasted in excess of 800 hours with less than 10 percent failure rate. Once the reversion issue is solved, this material holds much promise.

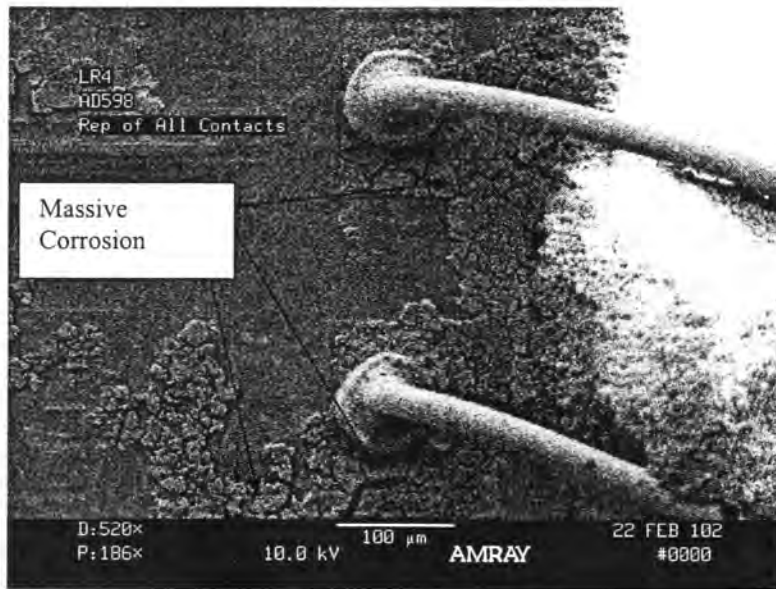


Figure 27. Typical Bond Pad Corrosion of Sample LR-4

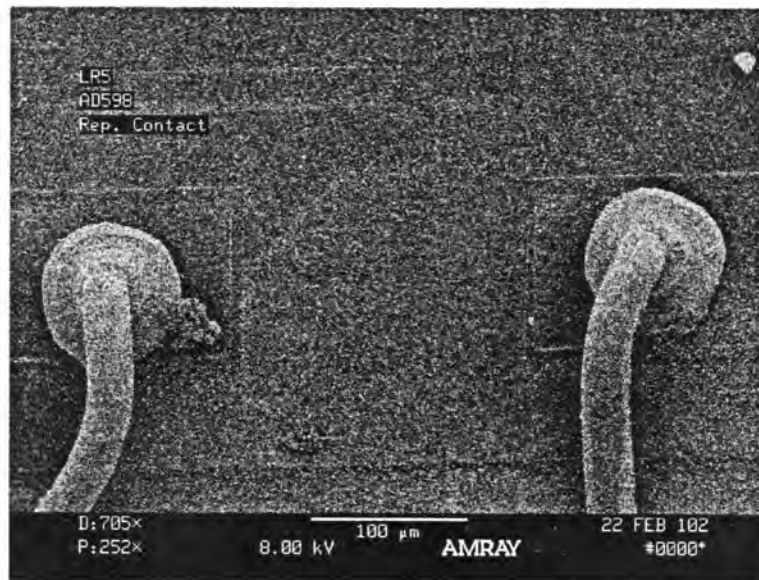


Figure 28. Typical Bond Pad Corrosion of Sample LR-5

Sample LA1 encapsulant parts decapsulated were samples LA1-2 and LA1-3. The LA1-2 sample was removed from plasma etch for analysis with the AD598 die still covered in coating. The other dies were completely exposed, and it was thought that if the

package was to remain in plasma etching, environmental conditions may affect the already exposed pads. All other dies exhibited minimal to no corrosion presence. This included the biased pads, which is not what would be expected. It is a possibility that the chlorine content was low enough that the corrosion mechanism had not progressed to cause visible corrosion.

The LA1-3 sample also had an AD598 die still covered in coating when the device was removed for analysis. Again, the other dies were completely exposed, and it was thought that if the package was to remain in plasma etching, environmental conditions may affect the already exposed pads. The CMP04 die was also missing in this package. It was likely lost during decapsulation and not recovered. This sample had some corrosion to varying extents on all bond pads. Again, this included the bias pads, which is what would be expected.

Internal Device Analysis Discussion

The results showed unexpectedly widespread extents of corrosion on all devices after they were decapsulated. As the chlorine content was lowered, it was expected that corrosion would decrease on the bond pad surfaces. While Sample LA1 had less corrosion as compared to Sample LD, all samples exhibited a higher degree of corrosion than what was expected given such low chlorine contents. Samples LD7 and LR had significant corrosion on some bond pads, but the reversion of the encapsulant may be the reason corrosion was more pronounced. The reverted encapsulant (liquid state) would allow water and chlorine ions to move through the encapsulant much more easily. Corrosion seen on the bond pads from the devices covered by LD7 and LR should be discounted because of the reversion issue.

Another issue is the fact that some biased pads were corrosion-free while some unbiased pads were heavily corroded. For example, sample LD-2 had two positive biased and three -0.0 (grounded) biased pads corrosion free, and 44 of 58 unbiased pads were corroded. Sample LD-5 contained only 5 unbiased pads that were corrosion free. Samples LD7-3 and 4, LR-4 and 5, and LA1-2 and 3 all had evidence of corrosion on all

unbiased pads. This makes it clear that knowledge of the bias state of the pad is not sufficient to allow one to predict the occurrence of corrosion. Previous reported results [2] led to the expectation that biasing would accelerate the corrosion rate.

Prior to this study it was believed that using an encapsulant with less than 10 ppm of chlorine ions would almost eliminate the potential for corrosion within PEMs [14], even in conditions of high pressure and humidity. All the encapsulants used in this study were below this limit, so all samples should have had minimal corrosion present on the bond pads. This was obviously not the case, leading to the conclusion that (1) pressure and humidity play a more significant role than initially believed, especially in low ionic content encapsulants, (2) the 10 ppm ionic content level is simply incorrect, or (3) a combination of these.

Previous investigations have shown that only a minute amount of chlorine content is necessary to accelerate corrosion. In a study where the surface of gold pads with a 12 volt applied bias were contaminated with KCl, it was found that less than 1×10^{-7} grams/cm² of KCl caused significant corrosion [29]. For sample encapsulant LR, which had a chlorine content of 0.9 ppm, a simple estimation of the amount of chlorine ions can be obtained. The surface area of the devices present in these samples is approximately 3.16 cm² and the approximate volume of encapsulant required to cover this area is 0.05 cm³. Based on the approximate density for the encapsulant being 1.77 g/cm³, 7.75×10^{-7} grams of chlorine would be present in each device. When spread over the area of 3.16 cm², the chlorine ion density is approximately 1.45×10^{-7} grams/cm² for each BGA package, well over the minimum found in [29]. This simple analysis indicates that corrosion may be expected even at the low values used in this study. While [29] used a bias of +12 volts, the results of the present study showed no strong correlation between corrosion and applied bias. This may indicate that the non-uniform nature of the corrosion seen when the samples were de-capsulated is a result of regions where the local concentration of chlorine is higher, causing a more rapid attack. Other mechanisms, or multiple mechanisms, not studied in [29] are also possible and these are discussed briefly below.

While chlorine content, humidity, and bias is the predominant factor producing corrosion on the bond pads within the devices [14], the data gathered from the de-capsulation process of the sample devices in this study has clearly shown that other factors or mechanisms are also involved. One factor held constant in this study that might be responsible is bond pad corrosion resulting from the presence of bromine ions. The corrosion mechanism in this case is believed to evolve in the following manner [28]:

- Bromine ions were freed from methyl bromide (CH_3Br) or of hydrogen bromide (HBr) from breakdown products of the resin:

$$\text{HBrCH}_3\text{Br} \Rightarrow \text{CH}_3^+ + \text{Br}^- \text{ or } 4\text{HBr} + 2\text{O} \Rightarrow 4\text{Br}^- + 2\text{H}_2\text{O}$$
- The bromine ion reacts with the aluminum in the gold-aluminum (Au_4Al) intermetallic phase, forming aluminum bromide (AlBr_3) and gold:

$$\text{Au}_4\text{Al} + 3\text{Br}^- \Rightarrow \text{AlBr}_3 + 4\text{Au}$$
- The aluminum bromide oxidizes, and this oxidation reaction provides the driving force until the Au_4Al intermetallic is consumed. The bromine ion is freed again and can continue to completely corrode the bond pad:

$$2\text{AlBr}_3 + 3\text{O} \Rightarrow \text{Al}_2\text{O}_3 + 6\text{Br}^-$$

However, since the presence of the intermetallic Au_4Al is uncommon [28], it is unlikely that this mechanism is occurring to a significant extent. It is interesting to note that the bromine ion is freed in the last reaction to continue the corrosion process [14], as is the case for the mechanism based on the chlorine ion. This would indicate that since neither ion is ever completely tied up in a reaction product, corrosion may be slowed, but it can never be eliminated.

Another potential corrosion mechanism is phosphorous related. Excess phosphorous oxide from the silicone dioxide insulating film can combine with high levels of humidity. This results in the production of phosphoric acid, which will lead to corrosion of the metallized region on the bond pads [13]. The possibility of this mechanism occurring could be verified by subjecting samples to HAST testing at varying degrees of humidity. Time and funding considerations did not allow for this possibility to be tested.

Based on the results and all possible alternate corrosion mechanisms reported in the literature it appears that the corrosion seen in the samples is related to the ionic content present in the samples. However, having said that it must be realized that at such low levels of chlorine content, the local environment surrounding a bond pad is critical in determining whether corrosion does or doesn't proceed on any specific pad. It is inferred from the present results that bias plays a minor role in corrosion. This would suggest that conditions exist locally that overcome any bias effects. These conditions may be a slight variation in ionic availability due to variations in chemistry, thickness, or moisture (which can be related to thickness also). An unbiased pad with a thinner layer of encapsulant may allow moisture to accelerate corrosion. On the other hand, a pad where the encapsulant layer is thicker may provide a greater ionic content, also accelerating corrosion. Measuring average ionic contents and average humidity conditions in a test chamber therefore does not accurately reflect the local conditions present at the pad surface. An experimental matrix involving a series of test blanks where the coating thickness is varied, as well as humidity and pressure, would be useful in trying to isolate the effects of the test parameters.

Given that the ion is never tied up in a reaction it is believed that eventually all pads will corrode due to one or more of the corrosion mechanisms. The corrosion of any individual pad will only be avoided as long as the local conditions are prevented, and diffusion of moisture and chlorine ions prevents this from being completely stopped. It is also believed that moisture will provide a path for electrical and ionic migration allowing corrosion to affect the unaffected pads. Once these mechanisms begin the only way to stop it is to remove the moisture and/or the ionic contaminant. Since moisture will always be present in service of these devices, tying up the ionic contaminant in some way is the most promising way to decrease overall corrosion.

CHAPTER 4. CONCLUSIONS

The goal of this research was to determine what level of chlorine content is permissible in an encapsulant that can be qualified as hermetic equivalent, thus passing 1000 hours HAST with less than 5% failure rate. Four potential candidate samples were evaluated: 1) Sample LD, FP 4450 Control Sample; 2) Sample LD7, FP4450HF; 3) Sample LR, “Cleanest Commercial Resin”; 4) Sample LA1, “Ion Getter. The following conclusions were reached:

- All observed samples had corrosion failures even at the lowest chlorine content sample. This indicates that if a minimum threshold for chlorine content exists, it is below the lowest samples tested.
- None of the encapsulants achieved hermetic equivalence.
- The bias state, contrary to what is believed, did not play as important role in the corrosion mechanism as the presence of chlorine and water. This is event with the fact that corrosion occurred at sites not directly biased and at times did not occur on site that were biased.
- While failures were reduced by using materials with less chlorine, corrosion was still present and proceeding without causing electrical failures, so other corrosion mechanisms must be causing some of the corrosion in the devices.
- FP4450HF and the “commercially cleanest resin” FP4450HF formulations experienced a break down in the encapsulant after about 600 hours of HAST; the encapsulant tended revert to its previous state (liquefy in high humidity) and flow out of the package. These materials must be reformulated to prevent this occurrence before further consideration.

Future Research

Additional research is recommended to further study this subject:

- Study lower chlorine content encapsulants, encapsulant thickness, very bromide and sodium content, evaluate corrosion trends based on sample die location in package, and bond pad size.

REFERENCES

- [1] Hawes, A. and Adams, T., "Systems Designers Should Take Care When Specifying Plastic Parts in Military Electronics," *Military Aerospace Magazine*, August 2000.
- [2] Hagge, J., "ROBOCOTS: A Program to Assure Robust Packaging of Commercial-Off-The-Shelf Integrated Circuits," *International Journal of Microcircuits and Electronic Packaging*, Issue IV, Vol. 23, No. 4, 2000.
- [3] Robock, P. V., and Nguyen, T. T., "Plastic Packaging," Chapter 8, Microelectronics Packaging Handbook, Editors: R. Tummala and E. Rymaszewski, Van Nostrand Reinhold, New York, pp. 540-649, 1989.
- [4] Bolger, J. C., "Die Attach and Encapsulation," *ISHM Short Course Notes*, Boston, MA, pp. 14-28, November 1994.
- [5] Selig, O., et al, "Corrosion in Plastic Packages: Sensitive Initial Delamination Recognition," *IEEE Trans. CPMT*, Part B, Vol. 18, No. 2, pp. 353-357, May 1995.
- [6] Analog Devices Inc., ADI Reliability Handbook, Norwood, MA, 2000.
- [7] Gottesfeld S. and Schultz, W., "Frequently Asked Questions About PEM Reliability," *PEM Consortium Presentation*, October, 2000.
- [8] Gottesfeld S. and Schultz, W., "Reliability Considerations for Using Plastic-Encapsulated Microcircuits in Military Applications," *Harris Semiconductor Corp.*, September, 1994.
- [9] National Semiconductor Corp., "Package Reliability," August 1999.
- [10] Gallace, L. and Rosenfield, M., RCA Review, Vol. 45, June 1984.
- [11] Lycoudes, N., Solid State Technology, No. 10, October 1978.
- [12] Stroehle, D., IEEE Trans. on Component Hybrids and Manufacturing Technology, CHMT-6, No. 4, December 1983.
- [13] Shumay, W. Jr., "Corrosion in Electronics," *Advance Materials and Processes Inc. Metal Progress*, September 1987.
- [14] Harmon, G., Wire Bonding in Microelectronics, McGraw-Hill, New York, 1989.

- [15] Hagge, J., et al, "Environmental Testing Results for Task 1 of the WASPP Program 846B Mutichip Module BGA Demonstration Vehicles," Rockwell Collins Working Paper WP02-2009, 2002.
- [16] Wichgers, J., "Final Report, Fly-By-Wire (FBW) Technology Development Project, FY 1999," Collins proprietary internal document for Boeing dated September 2000.
- [17] Livingston, H., "SSB-1: Guidelines for Using Plastic Encapsulated Microcircuits and Semiconductors in Military, Aerospace and Other Rugged Application."
- [18] Nelson, W., "Accelerated Testing: Statistical Models, Test Plans, and Data Analysis," John Wiley & Sons, 1990.
- [19] M. Brizoux, G. Deleuze, R. Digout and M. Nallino, "Plastic Encapsulated ICs in Military Equipment Reliability Prediction Modeling," Quality and Reliability Engineering International, Vol. 8, pp. 195-211, 1992.
- [20] Peck, D. "Comprehensive Model for Humidity Testing Correlation," 24th Annual Proceedings of the International Reliability Physics Symposium, IEEE, pp. 44-50, 1986.
- [21] Test Method A113-A, "Preconditioning of Plastic Surface Mount Devices Prior to Reliability Testing," JEDEC Standard JESD22-A113-A, Electronic Industries Association, June 1995.
- [22] Robock, P. V., and Nguyen, T. T., "Plastic Packaging," Chapter 8, in Microelectronics Packaging Handbook, Editors: R. Tummala and E. Rymaszewski, Van Nostrand Reinhold, New York, pp. 540-649, 1989.
- [23] Onesti, R., Rockwell Semiconductor Systems, personal communication, February 1990.
- [24] Hagge, J. "A Review of Moisture Consideration for ICs in Non-Hermetic Packaging," Rockwell Collins Working Paper WP99-2003, 1999.
- [25] Hagge, J. "ROBOCOTS: A Program to Assure Robust Packaging of Commercial-Off-The-Shelf (COTS) Integrated Circuits," Rockwell Collins Working Paper WP00-2007, 2000.
- [26] Hagge, J. and Wilcoxon, R. "ROBOCOTS Rapid Test Methods for Assessing Suitability of Commercial Plastic Package ICs for Use in Harsh Environments," Rockwell Collins Working Paper WP01-2026, 2001.

- [27] Harmon, G., Reliability and Yield Problems of Wire Bonding in Microelectronic, International Society for Hybrid Microelectronics, Reston, VA, 1991.
- [28] Ritz, K. N., Stacy, W. T., and Broadbent, E. K. "The Microstructure of Ball Bond Corrosion Failures," 25th Annual Proceedings of the IEEE Reliability Physics Symposium, pages 28-33, April 1987.
- [29] Oneida Recherche Services, "Why Be Concerned About Moisture in Hermetic Packages," 2000-2002.

APPENDIX

Non-corrosion failures were experienced throughout testing of the devices. The first example of non-corrosion failure is documented in Figure 29. Figure 29 shows electromigration growth which is present between two adjacent solder bumps. These issues developed due to bias and the presence of surface residues between the particular solder bumps.

As discussed earlier, some of the samples experienced a breakdown of the encapsulant material after prolonged HAST exposure. The epoxy went from a solid or cured form to a liquid state, seeping between seams in the dam as seen in Figure 30. This occurred after about the 500 hour point in HAST on sample encapsulants LD7 and LR.

The reversion did not cause any electrical test failures. The problem did become worse as HAST exposure increased. In many cases, the encapsulation came to the point that it resolidified and caused the sample to be glued into the test sockets. This damaged the test sockets, and the force required to remove the sample from the sockets split the laminate substrate from the top encapsulant, preventing any further electrical testing of these lots of test vehicles.

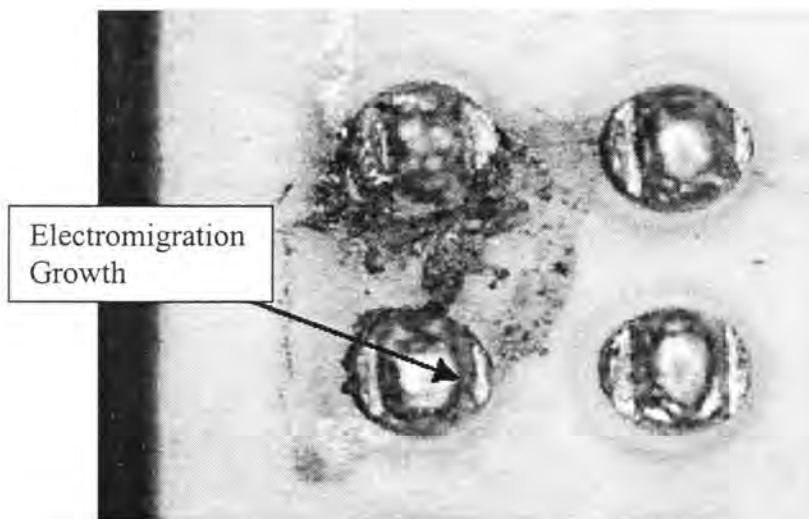


Figure 29. Electromigration Growth on the BGA Solder Bumps, 20X

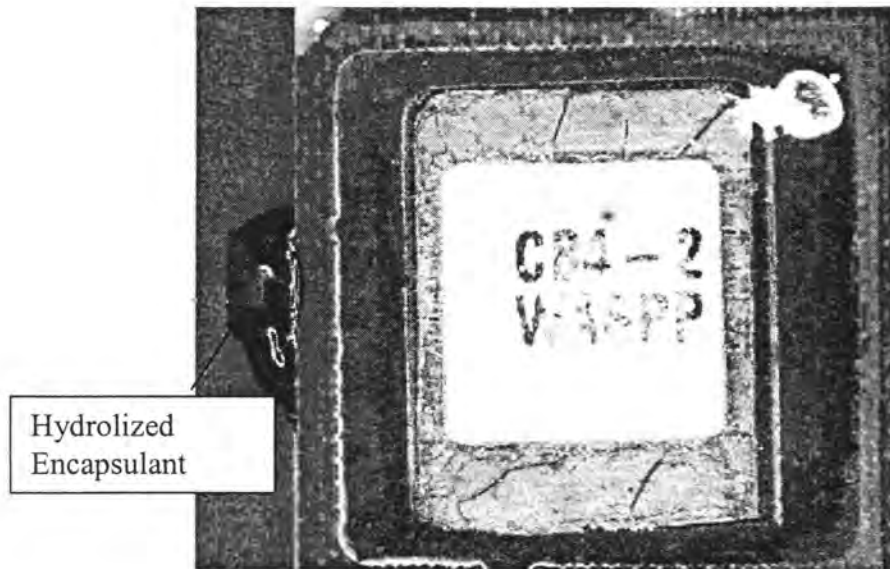


Figure 30. Encapsulant Leakage from Reversion, 10X

The last non-corrosion related failure occurred during electrical testing between HAST exposures. These resulted in failures either from the measured parameters being just marginally out of specification or due to contact resistance variations in the test sockets. These types of failures were quite evident because the data reported from exposure to exposure disappeared by the next test cycle. This was clearly not related to corrosion, so this data was removed from the final reports.